Hyperspectral Imaging Sensor with Real-time processor performing Principle Components Analyses for Gas Detection

March 2000

Michele Hinnrichs
Pacific Advanced Technology
PO Box 359
1000 Edison St.
Santa Ynez, CA 93460-0359
USA
Micheleh@syv.com

ABSTRACT

Chemical warfare agents in the gas phase are a considerable threat from terrorists anywhere there are enemy forces on a battle field. The ability to detect, identify and determine the direction of propagation of such gases is of considerable interest to the armed forces. With support from the US Air Force and Navy, Pacific Advanced Technology has developed a small man portable hyperspectral imaging sensor with an embedded DSP processor for real time processing that is capable of remotely imaging gas plums. Then, based upon their spectral signature the species and concentration levels can be determined. This system has been field tested at numerous places including White Mountain, CA, Edwards AFB, and Vandenberg AFB. Recently evaluation of the system for gas detection has been performed. This paper presents these results.

The system uses a conventional infrared camera fitted with a diffractive optic that images as well as disperses the incident radiation to form spectral images that are collected in band sequential mode. Because the diffractive optic performs both imaging and spectral filtering, the lens system consists of only a single element that is small, light weight and robust, thus allowing man portability. The number of spectral bands are programmable such that only those bands of interest need to be collected. The system is entirely passive, therefore, easily used in a covert operation.

Currently Pacific Advanced Technology is working on the next generation of this camera system that will have both an embedded processor as well as an embedded digital signal processor in a small hand held camera configuration. This will allow the implementation of signal and image processing algorithms for gas detection and identification in real time.

This paper will present field test data on gas detection and identification as well as discuss the signal and image processing algorithms used to enhance the gas visibility based on principal components analysis. We will also present data showing that the instrument can detect gases with a flow rate of less than 0.5 cubic feet per minute. Flow rates as low as 0.01 cubic feet per minute have been imaged with this system.

Report Documentation Page

Report Date	Report Type	Dates Covered (from... to)
00032000	N/A	-

Title and Subtitle Hyperspectral Imaging Sensor with Real-time processor performing Principle Components Analyses for Gas Detection	**Contract Number**
	Grant Number
	Program Element Number
Author(s) Hinnrichs, Michele	**Project Number**
	Task Number
	Work Unit Number
Performing Organization Name(s) and Address(es) Pacific Advanced Technology PO Box 359 1000 Edison St.	**Performing Organization Report Number**
Sponsoring/Monitoring Agency Name(s) and Address(es) Director, CECOM RDEC Night Vision and Electronic Sensors Directorate, Security Team 10221 Burbeck Road Ft. Belvoir, VA 22060-5806	**Sponsor/Monitor's Acronym(s)**
	Sponsor/Monitor's Report Number(s)
Distribution/Availability Statement Approved for public release, distribution unlimited	
Supplementary Notes The original document contains color images.	
Abstract	
Subject Terms	
Report Classification unclassified	**Classification of this page** unclassified
Classification of Abstract unclassified	**Limitation of Abstract** UNLIMITED
Number of Pages 14	

1.0 BACKGROUND

Pacific Advanced Technology is working on the development of a small, light weight, hand held imaging spectrometer with an imbedded image and data processor for real time processing of spectral images. The spectral imaging is based on our patented Image Multi-spectral Imaging (IMSS) technique.[1] This approach has been discussed in detail in previously published papers.[2,3,4,5] however, for clarity a brief discussion of the technique is given here.

The IMSS imaging spectrometer is a dispersive type. The basic concept for IMSS is shown in figure 1.0-1 where the IMSS approach is compared to a standard monochrometer. In a monochrometer the key elements are an entrance slit and exit slit along with a dispersing media such as a prism or grating. In order to obtain high resolution the entrance and exit slit must be very narrow thus reducing the optical throughput of the system. The light is dispersed perpendicular to the axis of the exit slit and spectrally scanned across this slit.

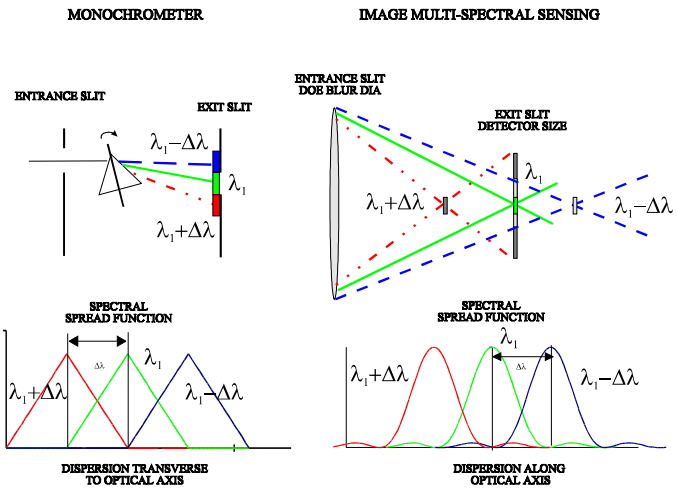

Figure 1.0-1 IMSS hyperspectral imaging used for spectro-radiometry.

In the IMSS approach the diffractive optical element disperses the light along the optical axis and the detector array/lens focal length is scanned to produce images of different colors. As shown in figure 1.0-1, when the detector lens spacing is such that the light from λ_1 is in focus, then light from the spectral bins on either side of λ_1 are out of focus. The advantage of this approach over a conventional dispersive spectrometer is that the entire input aperture collects the light as opposed to the narrow entrance slit and the throughput of the system is orders of magnitude higher than conventional dispersive system. Another advantage of this approach is that the photon shot noise comes from only a narrow spectral band as opposed to the entire spectral bandpass of the system as is the case for FTIR spectral imaging systems.

The design of the optics is such that the depth of spectral focus is very shallow so that spectral defocus takes place rapidly as the lens detector spacing is changed. The image that is produced is slightly blurred with the spectral component of interest in focus. Using proprietary image processing algorithms the out of focused image is rejected, and only the in focused component is retained (these algorithms can be implemented in real time using DSP's).

The lens/detector spacing is maintained using a standard stepper motor that scans from spectral bin to bin very rapidly. As an example, the instrument can scan from 3 to 5 microns sampling 880 spectral bins in 1

second (provided the camera is a high frame rate camera allowing 880 frames per second). The lens can be commanded to go to any spectral bin and dwell there indefinitely or a subset of the entire spectral region can be collected. The adaptability of the IMSS technology allows easy tuning for collection of only the spectral region of interest. The IMSS technology is extremely simple with all the dispersive and optical power designed in a single lens. The only moving part is a lead screw that drives the lens along the optical axis. This technology has proven to be very robust and has been field tested for hundreds of hours in all kinds of weather condition without a single failure. Because the system uses only a single lens it can be made very small and light weight for man portable and airborne applications.

This technology is currently being developed by Pacific Advanced Technology into the third generation where the infrared camera will use flexible electronics to allow enhancement of the small signals that are inherent in narrow band spectral images, and perform image and signal processing in real time with embedded digital signal processing hardware. A schematic of these electronics is given in figure 1.0-2 for reference. The electronics are made up of modules; 1) the sensor head module where the analog video is converted into a 14 bit digital signal, 2) the video buffer where nonuniformity correction and frame buffering is performed this module acts as the camera embedded frame grabber, 3) the display buffer where the video is reformatted for RS170 or LCD outputs, 4) the image processor where image and data processing is performed, and 5) the control processor with an embedded MBX860 uses a Windows CE operating system for command and control functions. There is also an interface to a visible camera where the infrared and visible image will be fused and displayed to the user.

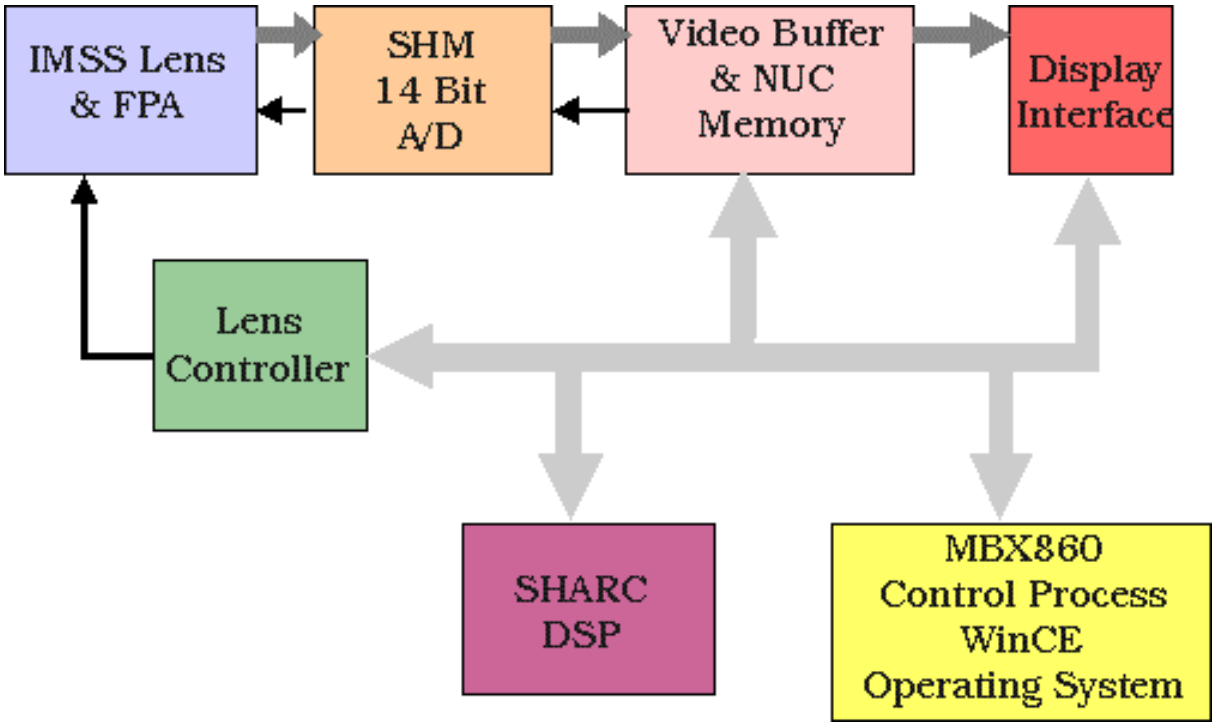

Figure 1.0-2. Third generation imaging spectrometer flexible electronics with embedded image and data processing.

2.0 DATA COLLECTION AND ANALYSIS

On December 21 and 22 1999 methane leak data was collected using the IMSS imaging spectrometer coupled to the HyPAT II data collection system. The image format is 256 x 256 pixels by two Bytes per pixel (resolution is only 12 bits). Two sets of data were collected, one of methane leaking from a pipe, and the second was methane leaking from below ground. The purposes of the two data collection exercises were; one to show that the IMSS can easily detect methane gas leaking from a pipe at flow rates less then 1 ft^3/min, and two to see if an underground leak could be detected using spectral image processing. In addition, statistical processing to enhance to above ground methane leak was used.

2.1 Above Ground Leaks

The data cubes looking at the methane leaking from a pipe were collected in step mode (vs scan mode) with a step resolution of 3, thus giving an image at about every resolution bin of the IMSS lens, as opposed to the data cubes looking for the underground leaks, which were collected in step mode with a step resolution of 1 giving about 3 samples for every spectral resolution bin.

The methane gas flow rate was measured and adjusted using a rotometer. Two data sequences were collected. The first with the building next door as the background and the second with the sky as a background.

Shown in figures 2.1-1 are two spectral images from one of the data cubes, the image on the left is centered at 4.6 microns (well out of the absorption band of methane) and the image on the right is centered at 3.4 microns (within the absorption band of methane). These images were taken from the baseline data cube where no gas is leaking from the pipe. The images have had the spectral blur removed by spatial deconvolution. Notice the difference in the pipe and background for these two bands. At 4.6 microns thermal differences dominate the image and at 3.4 microns solar reflection dominates the image. There is a magnification change between the data at 4.6 microns (left image) and that at 3.4 microns (right image). The data cubes were compensated for the magnification change prior to statistical analysis.

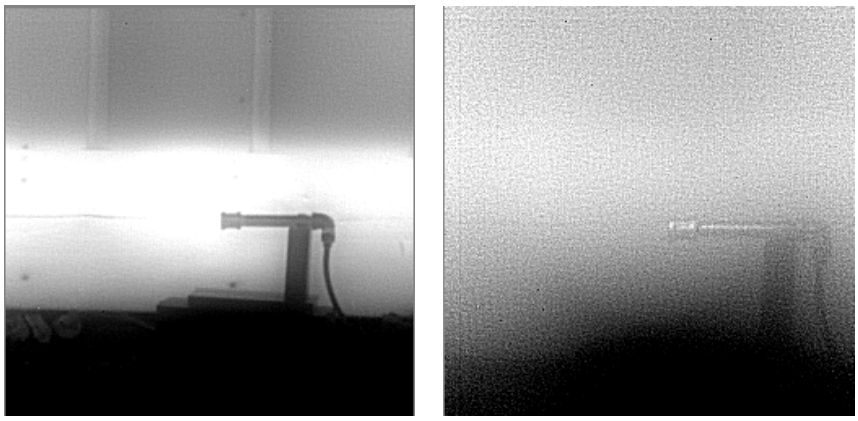

Figure 2.1-1. IMSS spectral images of the pipe and background used in the above ground leak test. Left image is at 4.8 microns and the right image is at 3.4 microns. No gas was leaking for these images.

An image at 3.4 microns with and without the leak is shown in figure 2.1-2. The data cube with no leak (image on left) and the data cube with the leak (image on the right) is shown with a very low flow rate of methane leaking at 0.5 ft^3/min. The display histogram is adjusted differently for these two images. In the image on the right the gas can barely be seen leaking from the pipe. The gas contrast with the background is very low on the order of 240 counts out of 4096 or about 6% of the dynamic range of the camera.

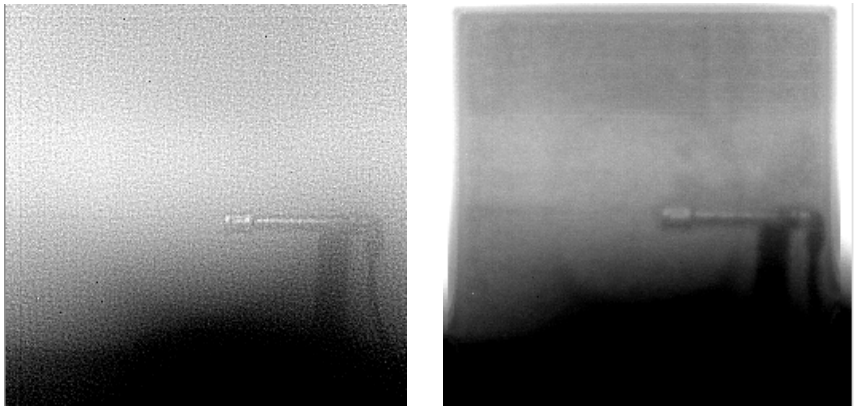

Figure 2.1- 2. Methane gas leaking from a pipe at 0.5 ft^3/min is shown in the image on the right. The image on the left has no leak

Using statistical image processing techniques the gas leak can be enhanced. Shown in figure 2.1-3 are three principal component images (3^{rd}, 4^{th}, and 6^{th}) where the gas leak shows up as a bright and/or dark plum emanating from the pipe. As the data cube was collected the plume was blown by the wind and thus was constantly changing direction during the period when the camera was tuned to the absorption band of methane explaining the different position of the plume in the principal component images.

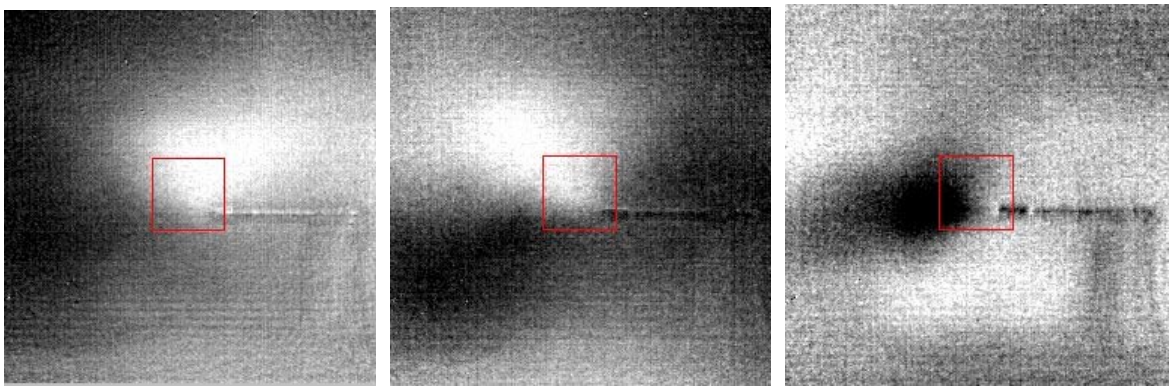

3^{rd} PC 4^{th} PC 6^{th} PC

Figure 2.1- 3. There principal component images of the methane gas leak at 0.5 ft^3/min.

Shown in figure 2.1- 4 is the gas plume painted in red and selected from end member data in an n dimensional scatter plot. End members in a scatter plot represent the purest pixels indicating different species in the hyperspectral scene. Even though the gas is optically thin and changing position during the hyperspectral data cube collection, the spices can be identified easily in an n dimensional scatter plot (for this case three colors were used, i.e. n is equal to 3). When viewing the principal component (PC) images the gas can be seen in many of the PC images as shown in figure 2.1- 5. Shown in figure 2.1-6 is principal component image 33 which is mostly dominated by white noise although some of the gas plume can still be seen. It is believed that the temporal nature of the plume allows it to appear deep into the principal component sequence.

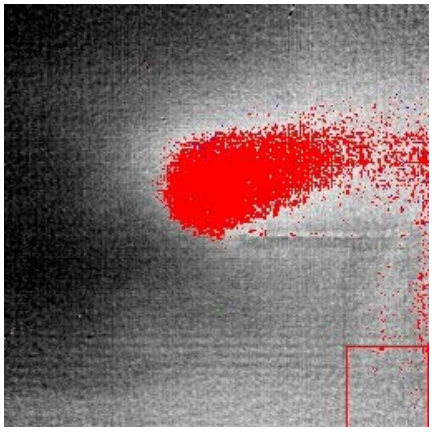

Figure 2.1- 4. Methane gas species detected from end member scatter plot.

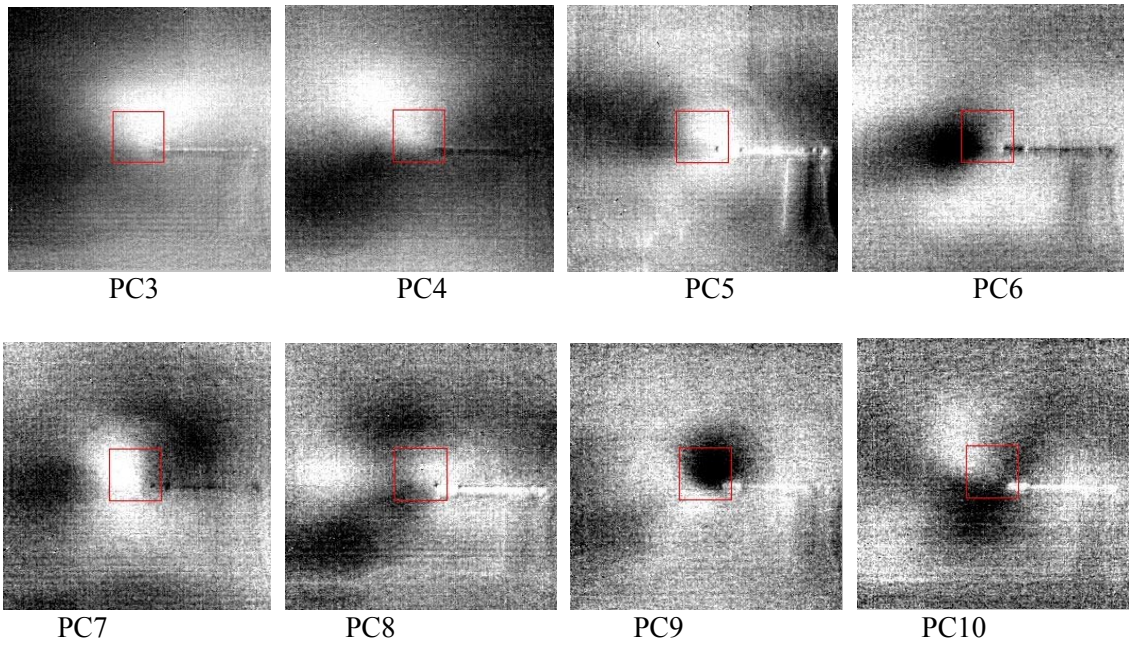

Figure 5. Showing principal component images 3 through 10 clearly indicate the presence of the methane gas leak.

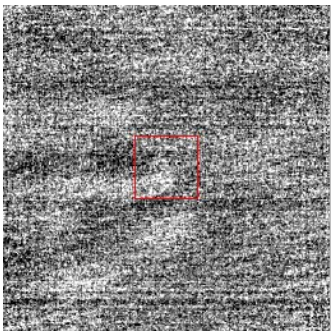

Figure 2.1- 6. Showing principal component image 33 where most of the scene is dominated by white noise although a small component of the gas plume can still be scene.

A data cube of 100 frames was collected with the IMSS imaging spectrometer tuned to 3.4 microns, in the center of the absorption band for methane. Again, statistical analysis of the image data was performed and again the plume is clearly seen in the principal component bands as shown in figure 2.1- 7. For this data sequence the wind was much stronger than for the previous sequence and the gas was blown to the right immediately after leaving the pipe.

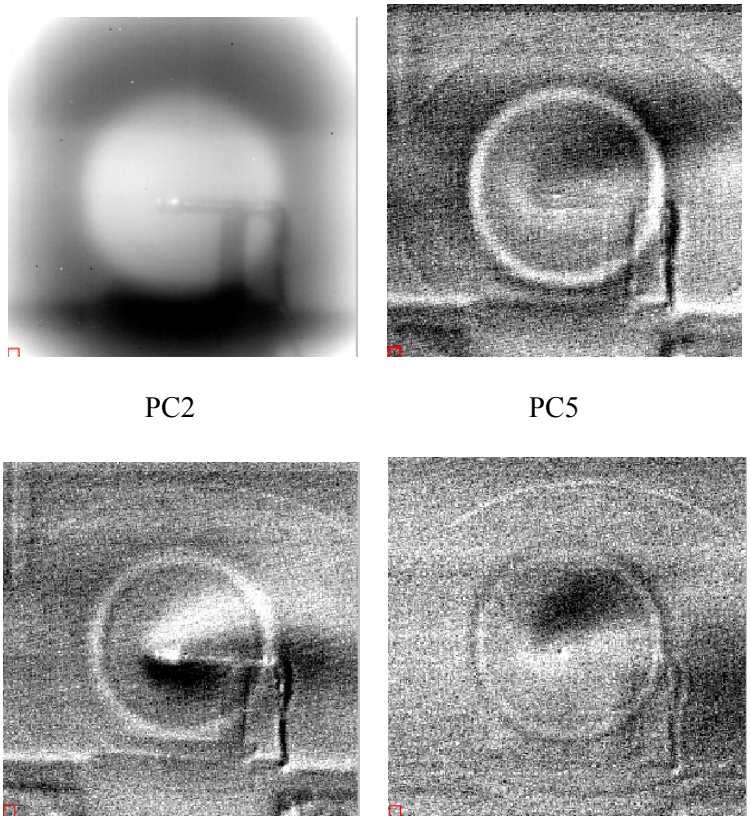

Figure 2.1- 7. Four principal component images of methane gas leaking where the IMSS was set at 3.4 microns and 100 frames of data was collected.

The circular artifact in the images is caused by using the internal flag in the infrared camera to perform the nonuniformity correction for the focal plane array. In doing so the non-uniformity from the lens and reflected cold shield can be seen after principal component analysis. If an external source is used to correct the nonuniformities in the focal plane array response then these artifacts are not present in the image.

For the two cases: first collecting band sequential image data (from 3 to 4 microns) at the frame rate of the camera of 60 frames per second, i.e. sampling the scene every 16.6 msec in a different spectral bin, and second tuning the camera for one spectral bin (3.4 microns) and collecting 100 frames at 16.6 msec intervals, the methane gas leak is clearly visible after principal component analysis. This is due to the temporal nature of the gas plume. While this same technique might not work for static targets, it works well for time varying targets provided the proper spectral bands are selected.

2.2 Underground Methane Leak

Data was collected on a methane leak that was buried under ground at a depth of 12 inches. An image of the disturbed earth and the tube that was used to transport the gas to the simulated underground leak is shown in figure 2.2-1 as well as an enlarged image of the section showing the surface area above the buried tubing used to transport the methane gas below ground. A rock of about four inches in length was placed above the leak area which is shown in the close up image.

a. b.

Figure 2.2- 1. A visible image of the underground gas leak.

Spectral data cubes were collected using the HyPAT II imaging spectrometer system with the IMSS lens operated in step mode scanning from 3 to 5 microns with a step resolution of 1, thus giving a data cube consisting of over 500 frames and over sampling the resolution by a factor greater than two. Data was collected on two different days. The first data collection was the same day that the hole was dug (December 12, 1999), and the second data collection was eleven days later after the moisture on the surface had dried up considerably. The difference in the disturbed soil (containing more moisture) and the undisturbed soil is noticeable in the visible image.

Shown in figure 2.2-2 are three images of the area above the ground gas leak. The upper image adjusted to have the same scale as the infrared images was taken with a visible digital camera. The image in the

lower left hand corner is a raw IMSS image at 4.8 microns before blur deconvolution. The image in the lower right hand corner is the same IMSS image after the Jan deconvolution process has been applied. These IMSS images are from the second data collection set eleven days after the earth was disturbed.

Visible Image

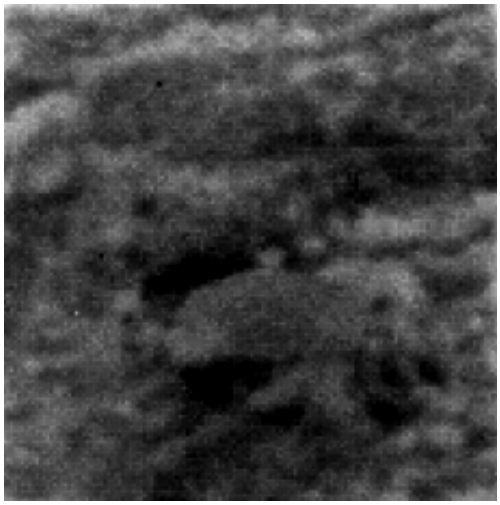

Raw IMSS at 4.8 microns Processed IMSS at 4.8 microns

Figure 2.2-2. Ground methane gas leak shown in the visible and infrared.

Using laboratory gas cells it was observed that spectra from weak signals could not be observed from the raw data. Using frame differencing with a gas cell containing nitrogen and the gas under test brought out the spectra clearly. Using this same strategy when looking for the underground methane gas leak we used two data cubes, one with and one without the gas leak for frame differenced.

Figure 2.2-3 is a group of images before and after frame differencing was applied. The upper two are taken at 4.8 microns the one on the left is with the methane gas leaking and the one on the right is not.

The image on the bottom left is the difference image of no leak (B) form leak (A), (A-B) where B is taken 2 minutes after A. The image in the lower right is the difference image of two data cubes taken eight minutes apart with no leak present. The intensity of the difference image has been offset, by a magnitude equal to the most negative value, to insure that all pixel values are a positive number. The brighter area indicates that the difference signal is larger and the darker area indicates a lower difference value or a reversal i.e. data cube B had a larger signal than data cube A. The area surrounding the rock, where the gas was leaking, shows a larger difference at 4.8 microns than the area away from the rock. The difference image with no leak has had the contrast stretched to bring out detail, for this case there are only 100 digital counts between black and white out of the full 12 bit image.

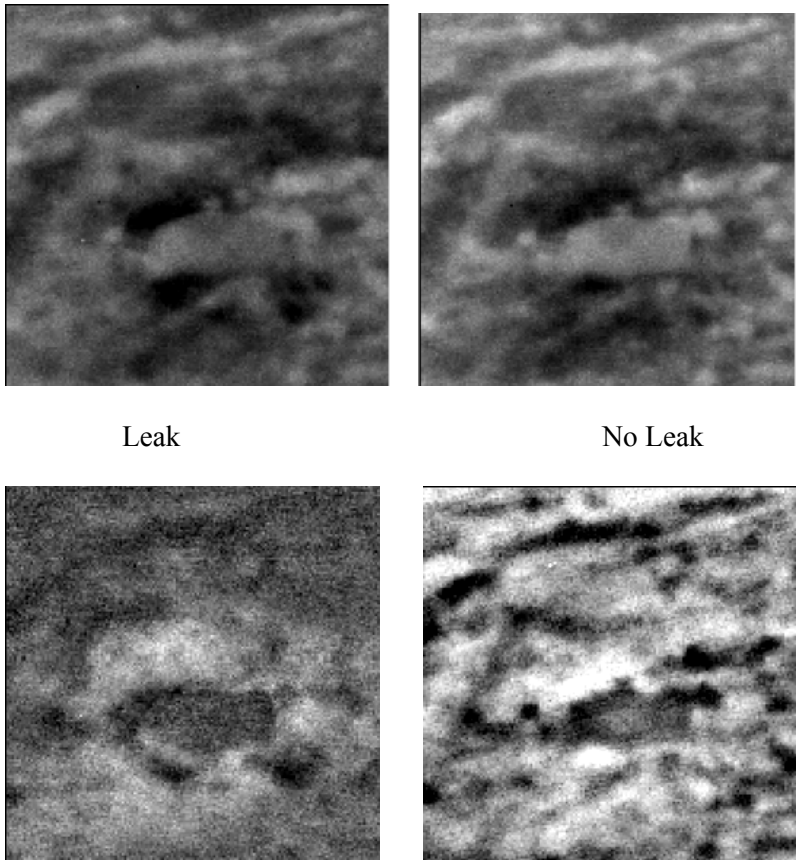

Leak No Leak

Difference Image With Leak Present Difference Image With No Leak

Figure 2.2-3. Images at 4.8 microns with and without leak and difference images.

Figure 2.2-4 again is the comparison of the IMSS images at 4.8 microns however, this time they are compared to an image of the 2nd and 3rd principal components of the difference images. The upper left image is taken at 4.8 microns from the data cube collected when no gas was leaking. The upper right is the same but taken 1 minute later after the gas had been turned on. The two data cubes with and without the gas leak were differenced on a frame by frame bases. Then statistical analysis was performed on the differenced data cube. The image in the lower left is the 2nd principal component of this difference data. The image in the lower left is the 3rd principal component. In both of these principal component images the area where the gas leak should have been is clearly different from the surrounding scene. For principal component images the brightness of the signal is not an indication of the absolute value of the original data because the intensity is now related to a new coordinate system based on the maximum

variance of the data. The dark area in the second principal component image indicates that the majority of the leak is observed in the region above the rock.

The bottom two images are principal components 2 and 3 of the difference of two data cubes where no leak was present. The data cubes where taken 8 minutes apart. The structure that can be seen in the 2nd PC is homogenous throughout the image and is most likely caused by differences in emissivity or reflectivity off the rock over the 8 minute interval between the two data cubes. The 3rd PC has no structure at all, and is dominated by noise as would be expected.

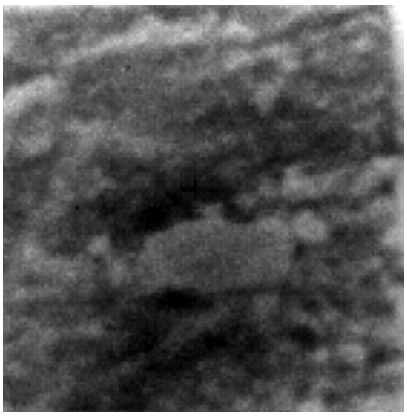

No leak

Leak

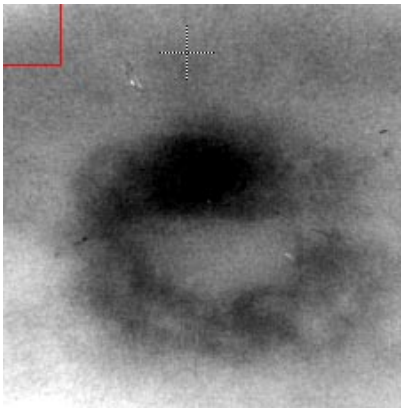

PC2 Leak Difference

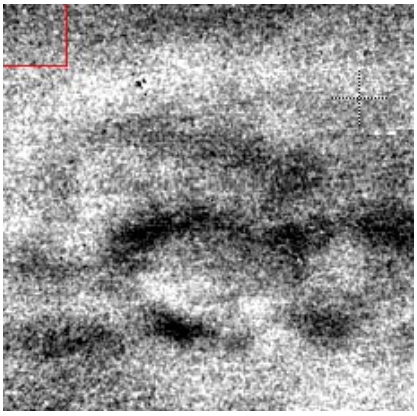

PC3 Leak Difference

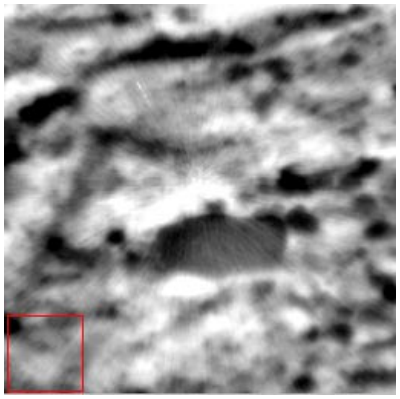

PC2 No Leak Difference

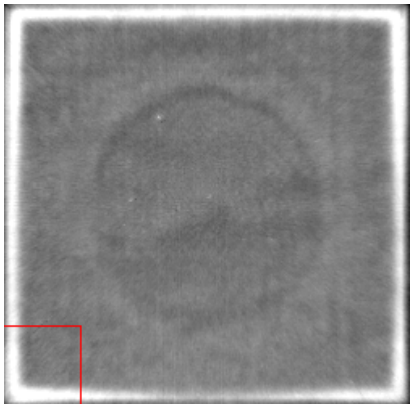

PC3 No Leak Difference

Figure 2.2-4. After differencing of the leak and no lead data cubes, and statistical analysis the gas leak is clearly visible in the 2nd principal component image. In comparison the difference of two no leak data cubes shows very different principal component images.

Spectra from pixels, on the rock, above the rock, and in the upper left corner are shown in figure 2.2-5. The absorption band of methane between 3.1 and 3.5 microns is shown by two vertical lines. Notice that there is considerable difference in the spectra in the region from 4.5 to 5 microns which is the carbon monoxide absorption band. The raw spectral which can be seen in the background has been fitted with a trend line which has been averaged over eight samples.

This spectra is a difference spectra, and a higher signal indicates a larger change, where a lower signal indicates a smaller change or a reversal. The spectra of the pixel above the rock has a larger change in the carbon monoxide absorption region than the pixel in the upper left corner of the image, or a pixel on the rock. The pixel above the rock shows a dip in the spectral region for methane absorption (3.1 to 3.5 microns). It is not known why the change in the carbon monoxide spectral region is greater for the pixel in the region where the gas is expected to be leaking from the ground. It is well understood that some methane gas is converted to CO_2 by microorganisms in the soil and is speculated that an oxygen depleted soil could cause methane to convert to CO.[6] The absorption of the atmosphere in the CO_2 spectral region would make it very difficult to see the methane converted to CO_2 .

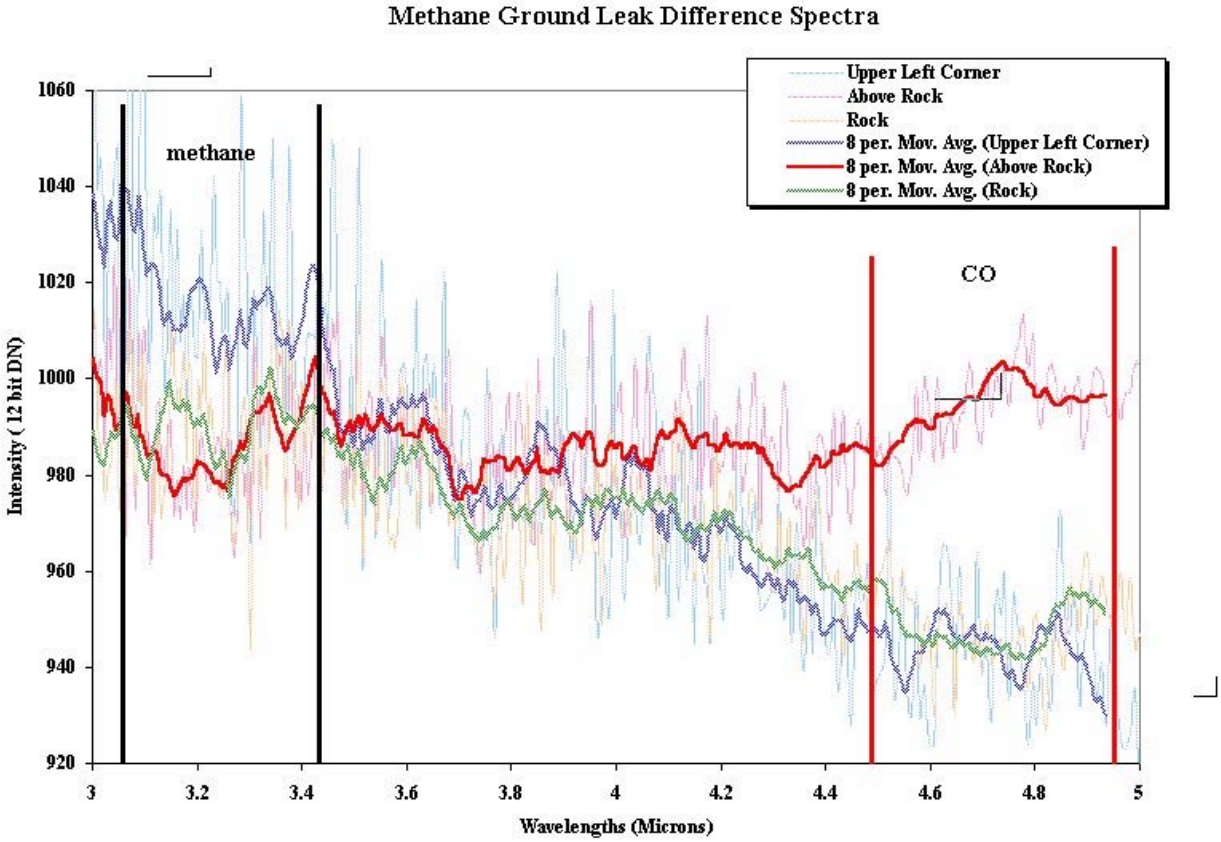

Figure 2.2-5. Sample spectra for the methane ground leak differenced data cube.

Shown in figure 2.2-6 is a larger statistical sampling of the area around the rock and the area out of the region where the gas was leaking. All pixels in the region above the rock, that correspond to the area indicated by the 2nd principal component where the gas leak should be, have a larger difference in the CO spectral region than those pixels away from the gas leak. The change spectra in the region of methane appears to be inconclusive.

In interpreting the difference spectra consider the horizontal line in the graph in figure 2.2-6. Signal above this line indicates a higher signal flux in the data cube with the methane leak, and signal below this line indicates a lower flux for the methane data cube. The spectral region from 3 to 4 microns has a higher infrared solar reflection than the region from 4 to 5 microns. The first is considered the solar band and the later is referred to as the thermal band of the midwave infrared region. The data would indicate that there is only a small change for most of the pixels in the methane absorption band, which is also the solar region, and fluctuations could be caused by a difference in the solar reflection on rocks from the two data cubes. However, in the carbon monoxide band, which is relatively insensitive to solar effects, the higher signal flux is most likely caused by a change in temperature. This temperature change could be the effect of carbon monoxide gas emanating from the soil due to the methane leak and interaction with micro-organisms in the soil.

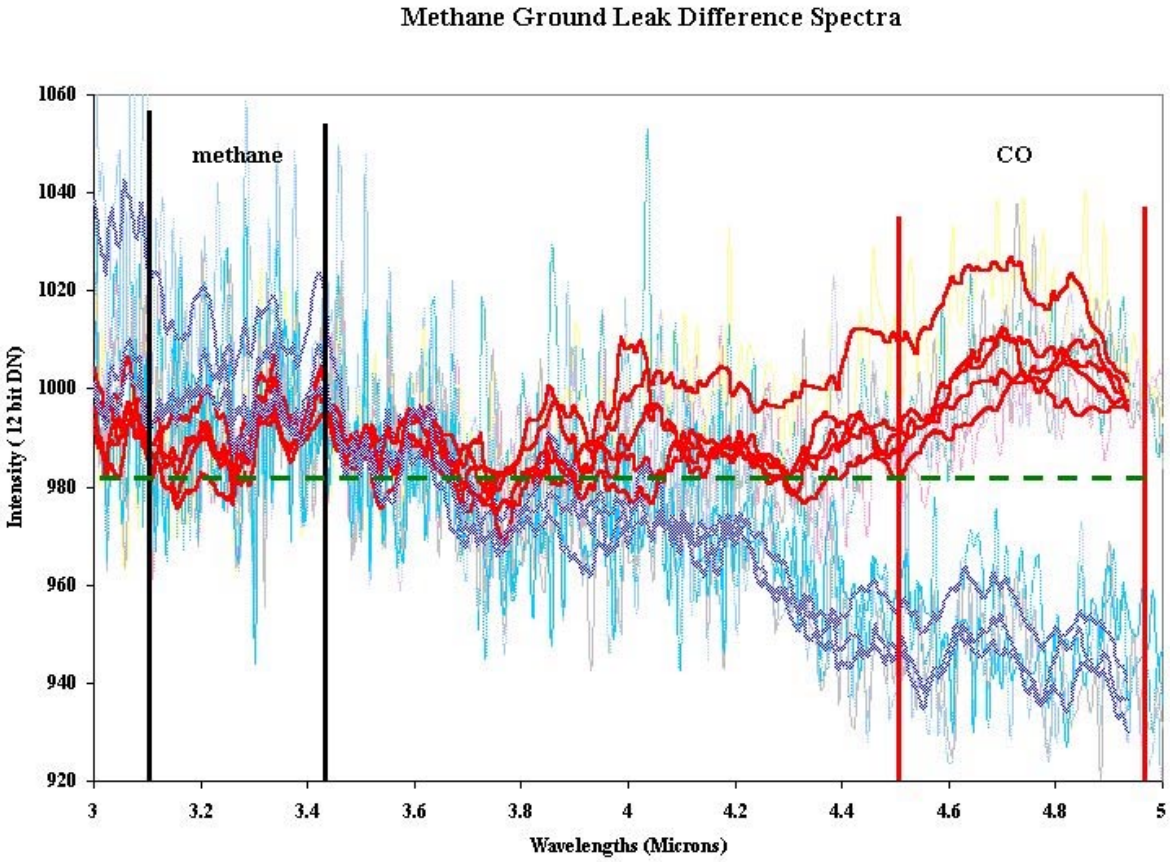

Figure 2.2-6. Spectral differences between the region above the rock and region in the upper portion of the image. The darker line (red) is above the rock.

3.0 CONCLUSION

Both above ground and below ground gas leaks have been successfully imaged using the IMSS imaging spectrometer and statistical image processing. For the above ground leak the dynamic and spectral nature of the gas was used to exploit the signal and enhance the image. It was determined that for both cases, one using a single spectral band tuned to the absorption of the gas, and two multiple sub-bands within the absorption band of the gas when statistical image processing is applied will enhance the visibility of the gas signal.

For the below ground leak it may be important to look throughout the entire spectral region to look for differences in the scene rather then to tune to the absorption band of the gas.

4.0 ACKNOWLEDGEMENTS

Although much of this work was performed with IR&D funding, Pacific Advanced Technology would like to acknowledge the support from the Office of Naval Research in the development of the IMSS technology that enabled this testing. In addition we would like to acknowledge the Department of Energy and the project manager Philip Goldberg for their support under a Phase I STTR that allowed some of this research to be performed. Pacific Advanced Technology would also like to thank the Gas Research Institute and Robert Lott for their support in understanding the phenomenon involved in the complex chemistry of the interaction of soil and gases.

---

[1] US Patent numbers, 5,479,258 and 5,867,264.

[2] Michele Hinnrichs, Mark Massie "New Approach to Imaging Spectroscopy Using Diffractive Optics", SPIE San Diego, July 1997.

[3] Michele Hinnrichs, Mark Massie, Buu Huynh and Brad Hinnrichs, "Hyperspectral Imaging Using a High Frame Rate Infrared Camera", International Symposium on Spectral Sensing Research, December 13-19 1997.

[4] Michele Hinnrichs "Remote Sensing for Gas Plume Monitoring Using State-of-the-art Infrared Hyperspectral Imaging", SPIE, Industrial and Environmental Monitors and Bio-sensors Nov 2-5, 1998.

[5] Michele Hinnrichs, "Imaging Spectrometer for Fugitive Gas Leak Detection", Industrial and Environmental and Industrial Sensing, SPIE, Boston September 19-20, 1999.

[6] Conversations with Robert Lott at the Gas Research Institute in Chicago, Illinois